

Peplomer bulb shape and coronavirus rotational diffusivity

Cite as: Phys. Fluids **33**, 033115 (2021); <https://doi.org/10.1063/5.0048626>


Submitted: 24 February 2021 . Accepted: 08 March 2021 . Published Online: 30 March 2021

 M. A. Kanso,  V. Chaurasia,  E. Fried, and  A. J. Giacomin

COLLECTIONS

Paper published as part of the special topic on [Flow and the Virus](#)

 This paper was selected as Featured

 This paper was selected as Scilight



View Online



Export Citation



CrossMark

ARTICLES YOU MAY BE INTERESTED IN

[Coronavirus rotational diffusivity](#)

Physics of Fluids **32**, 113101 (2020); <https://doi.org/10.1063/5.0031875>

[On coughing and airborne droplet transmission to humans](#)

Physics of Fluids **32**, 053310 (2020); <https://doi.org/10.1063/5.0011960>

[The novel Mechanical Ventilator Milano for the COVID-19 pandemic](#)

Physics of Fluids **33**, 037122 (2021); <https://doi.org/10.1063/5.0044445>

Physics of Fluids

SPECIAL TOPIC: Tribute to
Frank M. White on his 88th Anniversary

SUBMIT TODAY!



Peplomer bulb shape and coronavirus rotational diffusivity



Cite as: Phys. Fluids **33**, 033115 (2021); doi: 10.1063/5.0048626

Submitted: 24 February 2021 · Accepted: 8 March 2021 ·

Published Online: 30 March 2021



View Online



Export Citation



CrossMark

M. A. Kanso,¹ V. Chaurasia,² E. Fried,² and A. J. Giacomin^{1,3,4,a)}

AFFILIATIONS

¹Chemical Engineering Department, Polymers Research Group, Queen's University, Kingston, Ontario K7L 3N6, Canada

²Okinawa Institute of Science and Technology, Tancha, Onna, Kunigami District, Okinawa 904-0495, Japan

³Mechanical and Materials Engineering Department, Queen's University, Kingston, Ontario K7L 3N6, Canada

⁴Physics, Engineering Physics and Astronomy Department, Queen's University, Kingston, Ontario K7L 3N6, Canada

Note: This paper is part of the special topic, Flow and the Virus.

^{a)} Author to whom correspondence should be addressed: giacomin@queensu.ca

ABSTRACT

Recently, the rotational diffusivity of the coronavirus particle in suspension was calculated, from first principles, using general rigid bead-rod theory [M. A. Kanso, Phys. Fluids **32**, 113101 (2020)]. We did so by beading the capsid and then also by replacing each of its bulbous spikes with a single bead. However, each coronavirus spike is a glycoprotein trimer, and each spike bulb is triangular. In this work, we replace each bulbous coronavirus spike with a bead triplet, where each bead of the triplet is charged identically. This paper, thus, explores the role of bulb triangularity on the rotational diffusivity, an effect not previously considered. We thus use energy minimization for the spreading of triangular bulbs over the spherical capsid. The latter both translates and twists the coronavirus spikes relative to one another, and we then next arrive at the rotational diffusivity of the coronavirus particle in suspension, from first principles. We learn that the triangularity of the coronavirus spike bulb decreases its rotational diffusivity. For a typical peplomer population of 74, bulb triangularity decreases the rotational diffusivity by 39%.

Published under license by AIP Publishing. <https://doi.org/10.1063/5.0048626>

I. INTRODUCTION

Recently, we calculated the rotational diffusivity of the coronavirus particle in suspension as a function of peplomer population, from first principles, using general rigid bead-rod theory (Fig. 12 of Ref. 1). We did so by beading the capsid and then also by replacing each of its bulbous spikes with a single bead (Fig. 1). One of the challenges of *ab initio* calculations from general rigid bead-rod theory on coronaviruses is that the peplomer arrangement is not known. However, we do know that the spikes are charge-rich.^{2,3} It also seems reasonable to assume that they are charged identically. Furthermore, we know that the coronavirus spikes are not anchored into its hard capsid, but rather just into its elastic viral membrane (Sec. 1 of Ref. 4). The coronavirus spikes are, thus, free to rearrange under their own electrostatic repulsions. This is why coronavirus spikes normally present microscopically as uniformly distributed over the capsid. In our previous work, we followed the well-known polyhedral solutions to the Thomson problem for singly charged particles repelling one another over a spherical surface.⁵⁻⁷ By *Thomson problem*, we mean determination of how identically charged particles repel and then spread over a sphere by

minimizing system potential energy. This minimum system electrostatic potential energy, when divided by the sphere area, is not to be confused with surface energy.

Since each coronavirus spike is a glycoprotein trimer, each spike bulb is triangular (Fig. 14 of Ref. 1). By replacing each coronavirus spike bulb with a single bead (see circle in Fig. 14 of Ref. 1), our prior work neglects this triangularity. In this present work, we replace each bulbous coronavirus spike (Fig. 2) with a bead triplet (Fig. 3), with each bead identical and charged identically. We must, thus, replace the well-known polyhedral solutions to the single-bead Thomson problem with our new solutions to the triple-bead Thomson problem. In this work, we thus use minimum potential energy peplomer arrangements for our coronavirus model particles.

Since coronavirus bulbs are trimers, they not only translate into a set of centroidal positions relative to one another but also twist into a set of orientations relative to one another. Our potential energy minimization for our triply beaded peplomers thus yields both triplet positions and triplet orientations (Fig. 4). This new potential energy minimization yields a set of bead positions for the triply beaded

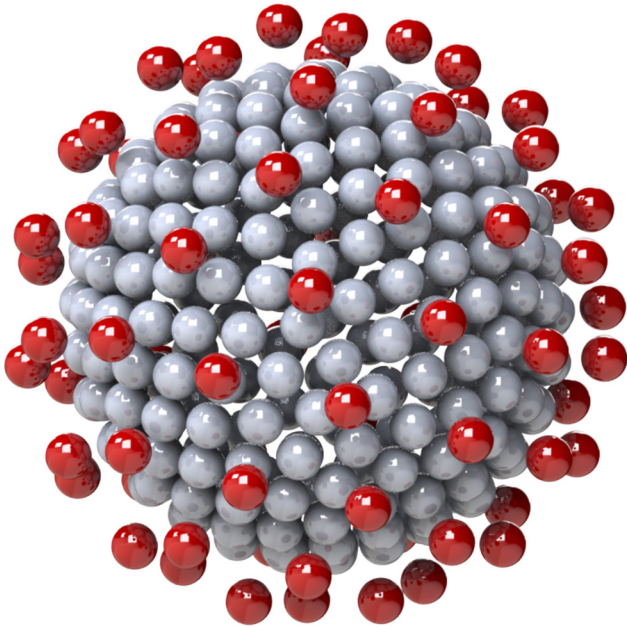


FIG. 1. General rigid bead-rod model of single beaded coronavirus, $N_c = 256$, $N_p = 74$ (row 1 of Table III).

peplomers whose centroid positions differ, of course, from the bead positions for the singly beaded counterpart of the same N_p . In other words, the polyhedra of centroids differ from the well-known Thomson solutions used in Ref. 1.

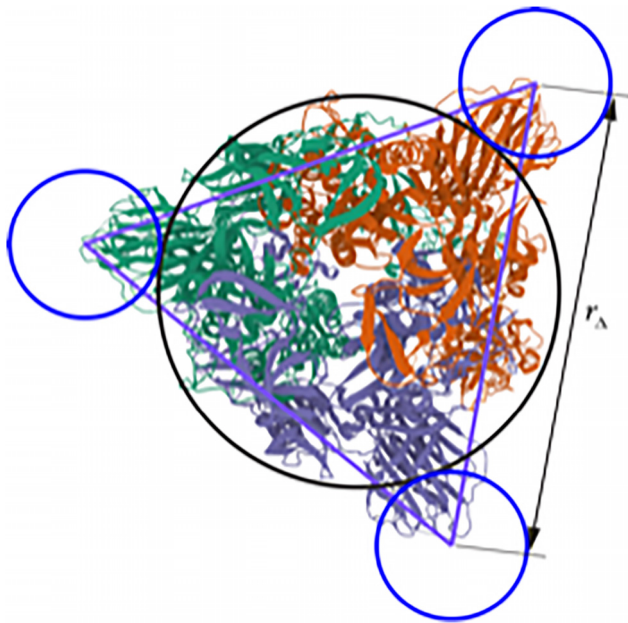


FIG. 2. This paper explores the role of bulb triangularity (three blue circles) on the rotational diffusivity. This improves upon the previously considered singly beaded bulb (black circle).¹ Bulb-end view of trimeric SARS-CoV peplomer (generated using 6CRZ.PDB data available from Ref. 15).

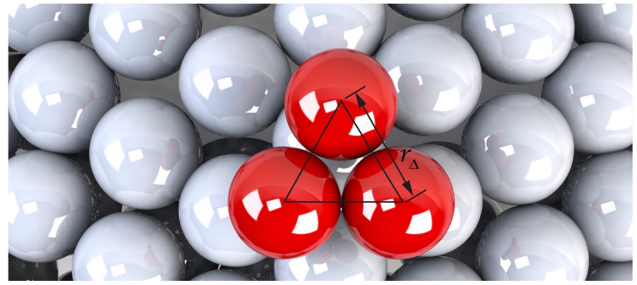


FIG. 3. General rigid bead-rod model of three beads peplomer head.

The challenge in determining the rotational diffusivity of a virus particle, from first principles, begins with modeling its intricate geometry with beads, locating the position of each bead. Once overcome, the next challenge is to use this geometry to arrive at the transport properties for the SARS-CoV-2 particle. From these, we deepen our understanding of how these remarkable particles align their peplomers both for long enough, and often enough, to infect.¹

Whereas our prior work relied on the Thomson solution for point charges (Fig. 1), here, we work with triads of point charges each spaced rigidly and equilaterally (Fig. 4). We, thus, complicate the energy minimization with the length of this equilateral triangle, r_Δ . From Table X of Ref. 1, mindful of Fig. 8 of Ref. 1, we get

$$\frac{1}{10} \leq \frac{r_\Delta}{r_p} \leq \frac{7}{25}, \tag{1}$$

and in this work, we choose $r_\Delta/r_p = 0.19$ for our energy minimization. To compare with our previous work, we match the dimensionless virus radius of Fig. 12 of Ref. 1, $r_v/r_c = 5/4$. Using the energy

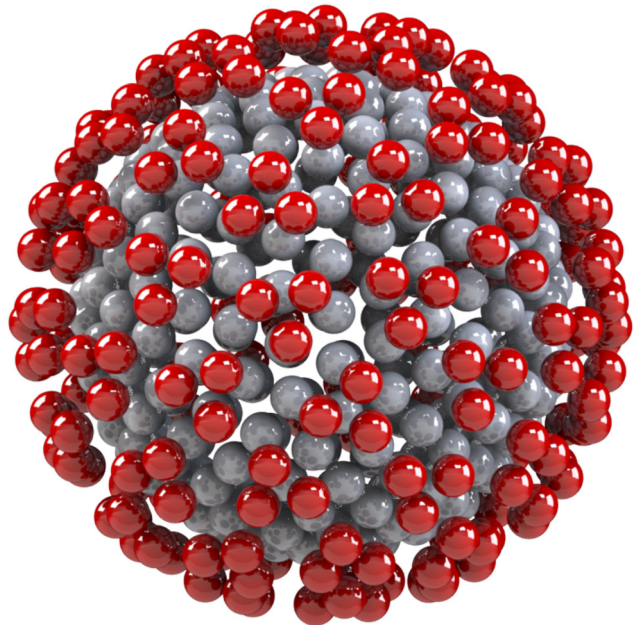


FIG. 4. General rigid bead-rod model of triple beaded coronavirus, $N_c = 256$, $N_p = 74$ (row 2 of Table III).

minimization to arrange and orient the coronavirus spikes relative to one another, we next arrive, from first principles, at the rotational diffusivity of the coronavirus particles with triple beaded peplomers in suspension.

II. METHOD

For this work, we chose general rigid bead-rod theory for its flexibility and accuracy (Sec. I of Refs. 8 and 9). Using general rigid bead-rod theory, we follow the method of Sec. II of Ref. 1 to construct our virus particles from sets of beads whose positions are fixed relative to one another. For example, the SARS-CoV-2 particle geometry is a spherical capsid surrounded by a constellation of protruding peplomers. We take our bead-rod models of virus particles to be suspended in a Newtonian solvent. To any such collection of bead masses, we can associate a *moment of inertia ellipsoid* (MIE) whose center is the center of mass and whose principal moments of inertia match those of the virus particle. The MIE, thus, determines the orientability of the virus particle, and thus, the virus rotational diffusivity. We use Eqs. (3)–(13) in Ref. 1 for the method of computing the rotational diffusivity (see Footnote 2 of p. 62 of Ref. 10)

$$D_r \equiv \frac{1}{6\lambda}, \quad (2)$$

or [Eq. (23) of Ref. 1]

$$\lambda_0 D_r = \frac{\nu}{72}, \quad (3)$$

which we will use for our results below. Symbols, dimensional, or non-dimensional are defined in Table I or Table II, following the companion paper for singly beaded peplomer for SARS-CoV-2 particle.¹

III. OSCILLATORY SHEAR FLOW

In this paper, we focus on small-amplitude oscillatory shear flow (SAOS). For this flow field, for the molecular definition of *small amplitude*, general rigid bead-rod theory yields [Eq. (32) of Ref. 1]

$$\lambda \dot{\gamma}^0 \ll \frac{1}{\nu\sqrt{2}}, \quad (4)$$

whose left side is the macromolecular Weissenberg number. The polymer contributions to the complex viscosity,^{11,12}

$$\eta^* \equiv \eta' - i\eta'', \quad (5)$$

are [Eqs. (40) and (41) of Ref. 8]

$$\frac{\eta' - \eta_s}{\eta_0 - \eta_s} = \left(\frac{1}{2b/a\nu} + 1 \right)^{-1} \left(\frac{1}{2b/a\nu} + \frac{1}{1 + (\lambda\omega)^2} \right), \quad (6)$$

and

$$\frac{\eta''}{\eta_0 - \eta_s} = \left(\frac{1}{2b/a\nu} + 1 \right)^{-1} \frac{\lambda\omega}{1 + (\lambda\omega)^2}, \quad (7)$$

where $\lambda\omega$ is the Deborah number. In this paper, we plot the real and *minus* the imaginary parts of the shear stress responses to small-amplitude oscillatory shear flow as functions of frequency, following Ferry (Secs. 2.A.4.-2.A.6. of Ref. 13) or Bird *et al.* (Sec. 4.4 of Ref. 14).

As $\omega \rightarrow 0$, for the polymer contribution to the zero-shear viscosity, we get

TABLE I. Dimensional variables.

Name	Unit	Symbol
Angular frequency	t^{-1}	ω
Bead diameter	L	d
Capsid radius	L	r_c
Complex viscosity	M/Lt	η^*
Dielectric permittivity	$T^4 I^2 / ML^3$	ϵ
Energy values in molecular-scale systems	ML^2/t^2	kT
Length of the equilateral triangle forming bead centers of triadic bulb	L	r_Δ
Length of the spike of each peplomer	L	ℓ
Minus imaginary part of non-linear complex viscosity	M/Lt	η''
Moments of inertia	ML^2	I_1, I_2, I_3
Number of dumbbells per unit volume	$1/L^3$	n
Peplomer bulb center radial position	L	$r_p \equiv r_v - r_b$
Peplomer sphere radius, $s = 1, 2, 3$	L	$r_{j,s}$
Peplomer vertex radius, $q = 1, 2, 3$	L	$r_{i,q}$
Point charge	As	Q
Real part of non-linear complex viscosity	M/Lt	η'
Relaxation time of rigid dumbbell	t	λ_0
Relaxation time of solution	t	λ
Rotational diffusivity	s^{-1}	D_r
Shear rate amplitude	t^{-1}	$\dot{\gamma}^0$
Solvent viscosity	M/Lt	η_s
Sphere radius	L	$r_s = r_c + \ell$
Temperature	T	T
Time	t	t
Total electrostatic energy	ML^2/t^2	E
Virus radius	L	r_v
Viscosity, zero-shear	M/Lt	η_0
Zero-shear first normal stress difference	M/L	$\Psi_{1,0}$

Legend: $M \equiv$ mass; $L \equiv$ length; $t \equiv$ time.

$$\frac{\eta_0 - \eta_s}{nkT\lambda} = \frac{a\nu}{2} + b = b \left[1 + \frac{2b}{a\nu} \right] \left(\frac{2b}{a\nu} \right)^{-1}, \quad (8)$$

which we use in the table of Sec. V below.

IV. MODELING OF TRIMERIC PEPLOMER

As shown by Kirchdoerfer,¹⁵ each trimeric peplomer head, consisting of three glycoproteins, is well-approximated by an equilateral

TABLE II. Dimensionless variables and groups.

Name	Symbol
Capsid-sphere	\mathcal{C}
Coefficient in Eq. (3)	ν
Coefficient in Eq. (6)	a
Coefficient in Eq. (6)	b
Deborah number, oscillatory shear	$De \equiv \lambda\omega$
Equilateral triangle of i_{th} peplomer	\mathcal{T}_i
Sphere	\mathcal{S}
Total number of beads	N
Total number of capsid beads	N_c
Total number of peplomers	N_p
Weissenberg number	$Wi \equiv \lambda\dot{\gamma}^0$

triangle when viewed along the spike axis. In the general rigid bead-rod model,¹ this trimer is replaced with a sphere. Here, we approximate the trimer by considering an identical point charge at each vertex of the equilateral triangle.

A. Kinematics

Let N_p be the number of trimeric peplomers attached to the capsid-sphere \mathcal{C} of radius r_c . Let \mathcal{T}_i denote the equilateral triangle that approximates the trimeric head of the i_{th} peplomer. Let the p_{th} vertex of \mathcal{T}_i be parameterized by $r_c r_{i,q}$, where $i = 1 \dots N_p$ and $q = 1, 2, 3$. Let the length of the side of \mathcal{T}_i , $i = 1 \dots N_p$ be given by d . Thus, the vertices of \mathcal{T}_i are

$$r_c^2 |r_{i,1} - r_{i,2}|^2 = r_c^2 |r_{i,1} - r_{i,3}|^2 = r_c^2 |r_{i,2} - r_{i,3}|^2 = d^2. \quad (9)$$

Let ℓ be the length of the spike of each peplomer, with each spike normal to \mathcal{C} at the point of contact on \mathcal{C} . We assume that the centroid of \mathcal{T}_i is at the other end of the spike. Therefore, it must lie on the sphere \mathcal{S} of radius $r_s = r_c + \ell$,

$$\frac{r_c^2 (r_{i,1} + r_{i,2} + r_{i,3})^2}{9} = r_s^2, \quad i = 1 \dots N_p. \quad (10)$$

We also assume that each triangle \mathcal{T}_i lies in the tangential plane of the \mathcal{S} at its centroid. This implies that normal to the plane of \mathcal{T}_i must align with the vector joining the centroid of \mathcal{T}_i to the center of \mathcal{S} ,

$$[(r_{i,1} - r_{i,2}) \times (r_{i,1} - r_{i,3})] \cdot (r_{i,1} + r_{i,2} + r_{i,3}) = 0, \quad (11)$$

which simplifies to

$$(r_{i,1} \times r_{i,2}) \cdot r_{i,3} + (r_{i,2} \times r_{i,3}) \cdot r_{i,1} + (r_{i,3} \times r_{i,1}) \cdot r_{i,2} = 0. \quad (12)$$

B. Energetics

Let each vertex of each triangle \mathcal{T}_i , $i = 1 \dots N_p$ be endowed with point charge Q . The total electrostatic energy of N_p peplomers, constrained to the sphere \mathcal{S} of radius r_c , is given by

$$E = \frac{Q}{4\pi\epsilon r_c} \sum_{i=1}^N \sum_{j=1}^N \sum_{q=1}^3 \sum_{s=1}^3 \frac{1}{|r_{i,q} - r_{j,s}|}, \quad (13)$$

where ϵ is the dielectric permittivity. Using the constrained minimization approach of Ref. 16, we obtain numerical equilibrium solutions $r_{i,q}$, $i = 1 \dots N_p$, and $p = 1, 2, 3$ that locally minimize the energy in Eq. (13) while satisfying the kinematic constraints in Eqs. (9)–(12), for given values of N_p . Since the charge Q appears only as a prefactor in Eq. (13), its value plays no role in determining equilibrium solutions.

Our trimeric model amounts to a replacement for the Thompson problem,⁵ the objective of which is to find a state that distributes N_p equilateral triads of charges over a unit sphere as evenly as possible, with minimum electrostatic energy. By contrast, Wales^{6,7} distributed N_p single charges, providing solutions for a large set of values of N_p .

V. RESULTS AND CONCLUSION

From Fig. 5, we learn that the detailed triangular structure of the peplomer head and its singly beaded counterpart share the same qualitative behavior. For both, the rotational diffusivity, $\lambda_0 D_r$, descends monotonically with N_p . However, the detailed triangular structure of the peplomer head reduces significantly $\lambda_0 D_r$ of the coronavirus particle. Specifically, at the measured peplomer population of $N_p = 74$, we see a reduction in $\lambda_0 D_r$ of 39%. On close inspection, Fig. 5 also reveals

$$\frac{\lambda_0 D_r(3N_p)}{\lambda_0 D_r(N_p)} \approx 1, \quad (14)$$

that is, the dimensionless rotational diffusivity of a coronavirus with N_p singly beaded peplomers has about the same dimensionless rotational diffusivity of a coronavirus with $\frac{1}{3}N_p$ triply beaded peplomers.

From Fig. 6, we learn that the elasticity, $\eta''/(\eta_0 - \eta_s)$, of the coronavirus particle suspension is slight and that the detailed triangular structure of the peplomer head slightly reduces this elasticity. From

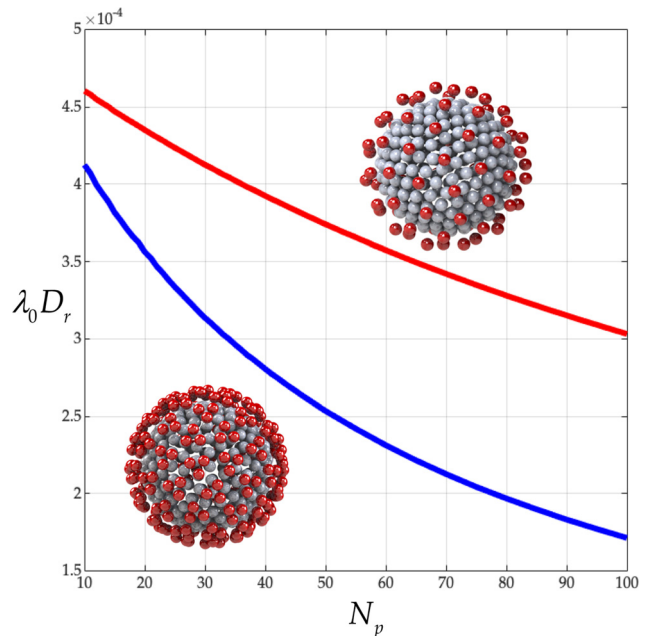


FIG. 5. Dimensionless rotational diffusivity $\lambda_0 D_r$ from Eq. (3) vs peplomer population N_p ($N_c = 256$): single (red) and triple beading (blue) corresponds to, respectively, rows 1 and 2 of Table III.

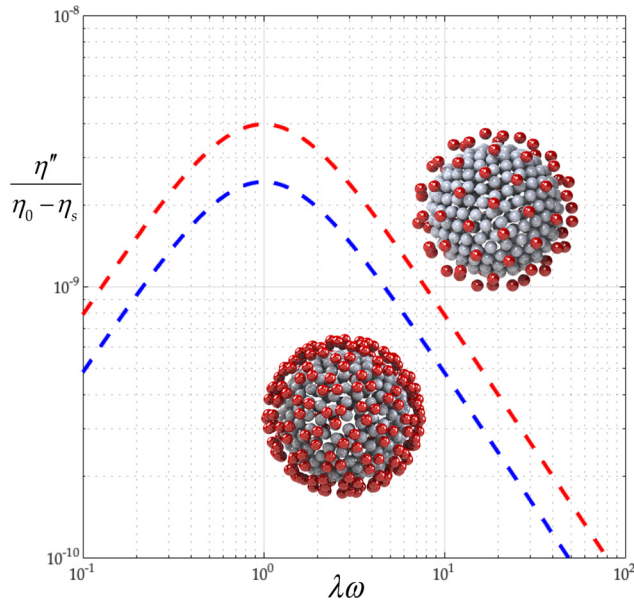


FIG. 6. Effect of single (red) and triple beading (blue) on *minus* the imaginary part of the complex viscosity ($N_c = 256$, $N_p = 74$ corresponds to, respectively, rows 1 and 2 of Table III). The polymer contribution $(\eta' - \eta_s)/nkT\lambda$ is nearly constant: $(\eta_0 - \eta_s)/nkT\lambda = 3/2$.

Table III, we see that the corresponding b is nearly zero so that the polymer contribution to the real part of the complex viscosity is constant, $(\eta' - \eta_s)/nkT\lambda = (\eta_0 - \eta_s)/nkT\lambda = 3/2$. From Table III, we learn that the detailed triangular structure of the peplomer head increases the relaxation time, λ , and thus, decreases the zero-shear viscosity, η_0 . From the rightmost column of Table III, we learn that the detailed triangular structure of the peplomer head decreases the zero-shear value of the first normal stress coefficient, $\Psi_{1,0}$.

Whereas much prior work on fluid physics related to the virus has attacked transmission,^{17–41} this paper focuses on the *ab initio* calculation of coronavirus transport properties. Specifically, we have determined the rotational diffusivity, the property governing the particle alignment for cell attachment (see Sec. I of Ref. 1). Although our work is mainly curiosity driven, it may deepen our understanding of drug, vaccine, and cellular infection mechanisms.

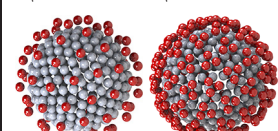
Chaurasia *et al.*⁴² (see also Chaurasia⁴³) developed a framework to find equilibrium solutions of a system consisting of flexible structures, specifically charged elastic loops constrained to a sphere. Their framework could be used to model flexible peplomers with uniformly charged heads. We leave this daunting task for a future study.

Since the coronavirus capsid can be ellipsoidal (Fig. 3. of Ref. 44), called *pleomorphism*, we must eventually consider this too. Whereas this work considered the detailed triangular structure of the peplomer head as triads of three point-charges, we could also consider uniformly charged triangular rigid peplomers constrained to a sphere. By *uniformly charged triangular*, we mean that the charge would be uniformly distributed over the edges of the triangle rather than point charges at its vertices. We leave this task for a later date.

One cognate transport problem is the transient translation and twist of coronavirus spikes rearranging freely under their own

TABLE III. Singly and triply beaded peplomer coronavirus particle characteristics from general rigid bead-rod theory.

Bulb beading	SARS-CoV-2	$\frac{f_c}{mL^2}$	$\frac{f_s}{mL^2}$	$\frac{f_p}{mL^2}$	a	b	ν	$\frac{2b}{av}$	$\frac{\eta_0 - \eta_s}{nkT\lambda}$	$\frac{\lambda}{\lambda_0}$	$\lambda_0 D_r$	$\frac{\Psi_{1,0}}{\lambda(\eta_0 - \eta_s)}$
	$N_c = 256, N_p = 74$	2.48×10^2	2.48×10^2	2.48×10^2	1.24×10^2	1.19×10^{-8}	2.42×10^{-2}	7.96×10^{-9}	$\frac{3}{2}$	4.96×10^2	3.36×10^{-4}	1.60×10^{-8}
	$N_c = 256, N_p = 74$	4.05×10^2	4.04×10^2	4.05×10^2	2.02×10^2	7.30×10^{-9}	1.50×10^{-2}	4.87×10^{-9}	$\frac{3}{2}$	8.09×10^2	2.06×10^{-4}	1.95×10^{-8}



electrostatic repulsions, for instance, the transient following the extraction of a single spike. This paper is, of course, silent on this interesting problem, which we leave for another day.

As in our previous work,¹ we have used repulsions of charged particles over the surfaces of spheres for both the capsid and the peplomer heads of the coronavirus to arrive at its transport properties. It has not escaped our attention that our solutions to the Thomson problem can also be used to calculate the Young's modulus of the coronavirus particle [Eq. (3a) of Ref. 45] and that by extension this Young's modulus will depend upon peplomer population. We leave this calculation for another day. When using the references cited herein, it is best to be mindful of corresponding ganged errata in Ref. 46.

ACKNOWLEDGMENTS

This research was undertaken, in part, thanks to the support from the Canada Research Chairs program of the Government of Canada for the Natural Sciences and Engineering Research Council of Canada (NSERC) Tier 1 Canada Research Chair in Rheology. This research was also undertaken, in part, thanks to the support from the Discovery Grant program of the Natural Sciences and Engineering Research Council of Canada (NSERC) (A. J. Giacomin), Vanier Canada Graduate Scholarship (M. A. Kanso), and the Mitacs Research Training Award (A. J. Giacomin and M. A. Kanso). A. J. Giacomin is indebted to the Faculty of Applied Science and Engineering of Queen's University at Kingston for its support through a Research Initiation Grant (RIG). V. Chaurasia and E. Fried gratefully acknowledge the support from the Okinawa Institute of Science and Technology Graduate University with a subsidy funding from the Cabinet Office, Government of Japan. We acknowledge Professor J. A. Hanna of the University of Nevada, Reno, for his help with Eq. (14).

DATA AVAILABILITY

The data that support the findings of this study are available within the article.

REFERENCES

- M. A. Kanso, J. H. Piette, J. A. Hanna, and A. J. Giacomin, "Coronavirus rotational diffusivity," *Phys. Fluids* **32**(11), 113101 (2020).
- Q. Yao, P. S. Masters, and R. Ye, "Negatively charged residues in the endodomain are critical for specific assembly of spike protein into murine coronavirus," *Virology* **442**(1), 74–81 (2013).
- R. Ye, C. Montalto-Morrison, and P. S. Masters, "Genetic analysis of determinants for spike glycoprotein assembly into murine coronavirus virions: Distinct roles for charge-rich and cysteine-rich regions of the endodomain," *J. Virol.* **78**(18), 9904–9917 (2004).
- M. A. Tortorici and D. Veesler, "Structural insights into coronavirus entry," *Adv. Virus Res.* **105**, 93–116 (2019).
- J. J. Thomson, "XXIV. On the structure of the atom: An investigation of the stability and periods of oscillation of a number of corpuscles arranged at equal intervals around the circumference of a circle; with application of the results to the theory of atomic structure," *London, Edinburgh, Dublin Philos. Mag. J. Sci., Ser. 6* **7**(39), 237–265 (1904).
- D. J. Wales and S. Ulker, "Structure and dynamics of spherical crystals characterized for the Thomson problem," *Phys. Rev. B* **74**(21), 212101 (2006).
- D. J. Wales, H. McKay, and E. L. Altschuler, "Defect motifs for spherical topologies," *Phys. Rev. B* **79**(22), 224115 (2009).
- M. A. Kanso, A. J. Giacomin, C. Saengow, and J. H. Piette, "Macromolecular architecture and complex viscosity," *Phys. Fluids* **31**(8), 087107 (2019); Editor's pick. Errata: Eq. (21) should be " $a^2\nu^2 + \frac{2}{3}(6b - 9)av + \frac{1}{3}(36b^2 - 123b + 81) = 0$;" in Table XIV, $n_0 - n_s$ should be $\eta_0 - \eta_s$. In Table XV, $\psi_{1,0}$ should be $\Psi_{1,0}$, and nKT should be nkT . In Table IV, Macromolecule 21 entry should be $[-\frac{1}{2}L, -\frac{\sqrt{3}}{2}L, 0]$; $[L, 0, 0]$; $[0, 0, 0]$; $[-\frac{1}{2}L, \frac{\sqrt{3}}{2}L, 0]$ and Macromolecule 17 entry should be multiplied by L . In Eq. (44), η'' should be $2\eta''$.
- M. A. Kanso, "Polymeric liquid behavior in oscillatory shear flow," Masters thesis (Polymers Research Group, Chemical Engineering Department, Queen's University, Kingston, Canada, 2019).
- R. B. Bird, C. F. Curtiss, R. C. Armstrong, and O. Hassager, *Dynamics of Polymeric Liquids*, 2nd ed. (John Wiley & Sons, Inc., New York, 1987), Vol. 2; Errata: On p. 409 of the first printing, the $(n + m)!$ in the denominator should be $(n + m)$; in Table 16.4–1, under L entry "length of rod" should be "bead center to center length of a rigid dumbbell," in the Fig. 14.1–2 caption, "Multibead rods of length L " should be "Multibead rods of length $L + d$."
- R. B. Bird and A. J. Giacomin, "Who conceived the complex viscosity?," *Rheol. Acta* **51**(6), 481–486 (2012).
- A. J. Giacomin and R. B. Bird, "Erratum: Official Nomenclature of The Society of Rheology- η " *J. Rheol.* **55**(4), 921–923 (2011).
- J. D. Ferry, *Viscoelastic Properties of Polymers*, 3rd ed. (Wiley, New York, 1980).
- Bird, R. B. R. C. Armstrong and O. Hassager, *Dynamics of Polymeric Liquids*, 1st ed. (Wiley, New York, 1977), Vol. 1.
- R. N. Kirchdoerfer, N. Wang, J. Pallesen, D. Wrapp, H. L. Turner, C. A. Cottrell, K. S. Corbett, B. S. Graham, J. S. McLellan, and A. B. Ward, "Stabilized coronavirus spikes are resistant to conformational changes induced by receptor recognition or proteolysis," *Sci. Rep.* **8**(1), 15701 (2018).
- J. Nocedal and M. L. Overton, "Projected Hessian updating algorithms for nonlinearly constrained optimization," *SIAM J. Numer. Anal.* **22**(5), 821–850 (1985).
- T. Dbouk and D. Drikakis, "On coughing and airborne droplet transmission to humans," *Phys. Fluids* **32**(5), 053310 (2020).
- R. Bhardwaj and A. Agrawal, "Likelihood of survival of coronavirus in a respiratory droplet deposited on a solid surface," *Phys. Fluids* **32**(6), 061704 (2020).
- S. Verma, M. Dhanak, and J. Frankenfield, "Visualizing the effectiveness of face masks in obstructing respiratory jets," *Phys. Fluids* **32**(6), 061708 (2020).
- T. Dbouk and D. Drikakis, "On respiratory droplets and face masks," *Phys. Fluids* **32**(6), 063303 (2020).
- S. Chaudhuri, S. Basu, P. Kabi, V. R. Unni, and A. Saha, "Modeling the role of respiratory droplets in Covid-19 type pandemics," *Phys. Fluids* **32**(6), 063309 (2020).
- Y. Y. Li, J. X. Wang, and X. Chen, "Can a toilet promote virus transmission? From a fluid dynamics perspective," *Phys. Fluids* **32**(6), 065107 (2020).
- G. Busco, S. R. Yang, J. Seo, and Y. A. Hassan, "Sneezing and asymptomatic virus transmission," *Phys. Fluids* **32**(7), 073309 (2020).
- R. Bhardwaj and A. Agrawal, "Tailoring surface wettability to reduce chances of infection of COVID-19 by a respiratory droplet and to improve the effectiveness of personal protection equipment," *Phys. Fluids* **32**(8), 081702 (2020).
- X. Wang, Y. Y. Li, X. D. Liu, and X. Cao, "Virus transmission from urinals," *Phys. Fluids* **32**(8), 081703 (2020).
- P. Prasanna Simha and P. S. Mohan Rao, "Universal trends in human cough airflows at large distances," *Phys. Fluids* **32**(8), 081905 (2020).
- J. Plog, J. Wu, Y. J. Dias, F. Mashayek, L. F. Cooper, and A. L. Yarin, "Reopening dentistry after COVID-19: Complete suppression of aerosolization in dental procedures by viscoelastic Medusa Gorgo," *Phys. Fluids* **32**(8), 083111 (2020).
- C. P. Cummins, O. J. Ajayi, F. V. Mehendale, R. Gabl, and I. M. Viola, "The dispersion of spherical droplets in source-sink flows and their relevance to the COVID-19 pandemic," *Phys. Fluids* **32**(8), 083302 (2020).
- M. R. Pendar and J. C. Páscoa, "Numerical modeling of the distribution of virus carrying saliva droplets during sneeze and cough," *Phys. Fluids* **32**(8), 083305 (2020).
- B. Wang, H. Wu, and X. F. Wan, "Transport and fate of human expiratory droplets—A modeling approach," *Phys. Fluids* **32**(8), 083307 (2020).
- H. De-Leon and F. Pederiva, "Particle modeling of the spreading of coronavirus disease (COVID-19)," *Phys. Fluids* **32**(8), 087113 (2020).
- S. Verma, M. Dhanak, and J. Frankenfield, "Visualizing droplet dispersal for face shields and masks with exhalation valves," *Phys. Fluids* **32**(9), 091701 (2020).

- ³³E. Hossain, S. Bhadra, H. Jain, S. Das, A. Bhattacharya, S. Ghosh, and D. Levine, "Recharging and rejuvenation of decontaminated N95 masks," *Phys. Fluids* **32**(9), 093304 (2020).
- ³⁴M. Vadivukkarasan, K. Dhivayaraja, and M. V. Panchagnula, "Breakup morphology of expelled respiratory liquid: From the perspective of hydrodynamic instabilities," *Phys. Fluids* **32**(9), 094101 (2020).
- ³⁵S. K. Das, J. E. Alam, S. Plumari, and V. Greco, "Transmission of airborne virus through sneezed and coughed droplets," *Phys. Fluids* **32**(9), 097102 (2020).
- ³⁶R. Mittal, C. Meneveau, and W. Wu, "A mathematical framework for estimating risk of airborne transmission of COVID-19 with application to face mask use and social distancing," *Phys. Fluids* **32**(10), 101903 (2020).
- ³⁷S. Kumar and H. P. Lee, "The perspective of fluid flow behavior of respiratory droplets and aerosols through the facemasks in context of SARS-CoV-2," *Phys. Fluids* **32**(11), 111301 (2020).
- ³⁸D. Fontes, J. Reyes, K. Ahmed, and M. Kinzel, "A study of fluid dynamics and human physiology factors driving droplet dispersion from a human sneeze," *Phys. Fluids* **32**(11), 111904 (2020).
- ³⁹S. Chaudhuri, S. Basu, and A. Saha, "Analyzing the dominant SARS-CoV-2 transmission routes toward an ab initio disease spread model," *Phys. Fluids* **32**(12), 123306 (2020).
- ⁴⁰J. Akhtar, A. L. Garcia, L. Saenz, S. Kuravi, F. Shu, and K. Kota, "Can face masks offer protection from airborne sneeze and cough droplets in close-up, face-to-face human interactions?—A quantitative study," *Phys. Fluids* **32**(12), 127112 (2020).
- ⁴¹H. Wang, Z. Li, X. Zhang, L. Zhu, Y. Liu, and S. Wang, "The motion of respiratory droplets produced by coughing," *Phys. Fluids* **32**(12), 125102 (2020).
- ⁴²V. Chaurasia, Y.-C. Chen, and E. Fried, "Interacting charged elastic loops on a sphere," *J. Mech. Phys. Solids* **134**, 103771 (2020).
- ⁴³V. Chaurasia, "Variational formulation of charged curves confined to a sphere," Ph.D. thesis (Department of Mechanical Engineering, University of Houston, Houston, Texas, USA, 2018).
- ⁴⁴N. Zhu, D. Zhang, W. Wang, X. Li, B. Yang, J. Song, X. Zhao, B. Huang, W. Shi, R. Lu, P. Niu, F. Zhan *et al.*, "A novel coronavirus from patients with pneumonia in China, 2019," *N. Engl. J. Med.* **382**(8), 727–733 (2020).
- ⁴⁵Bowick, M. A. Cacciuto, D. R. Nelson, and A. Travasset, "Crystalline order on a sphere and the generalized Thomson problem," *Phys. Rev. Lett.* **89**(18), 185502 (2002).
- ⁴⁶Kanso, M. A. V. Chaurasia, E. Fried, and A. J. Giacomin, "Peplomer bulb shape and coronavirus rotational diffusivity," PRG Report No. 076, QU-CHEE-PRGTR-2021-76 (Polymers Research Group, Chemical Engineering Dept., Queen's University, Kingston, Canada, 2021).